Published in final edited form as:

Gastroenterology. 2014 December ; 147(6): 1219–1221. doi:10.1053/j.gastro.2014.08.034.

Endoscopic Optical Coherence Angiography Enables Three Dimensional Visualization of Subsurface Microvasculature

Tsung-Han Tsai[1], **Osman O. Ahsen**[1], **Hsiang-Chieh Lee**[1], **Kaicheng Liang**[1], **Marisa Figueiredo**[2], **Yuankai K. Tao**[1], **Michael G. Giacomelli**[1], **Benjamin M. Potsaid**[1,3], **Vijaysekhar Jayaraman**[4], **Qin Huang**[2], **Alex E. Cable**[3], **James G. Fujimoto**[1], and **Hiroshi Mashimo**[2]

[1]Department of Electrical Engineering and Computer Science and Research Laboratory of Electronics, Massachusetts Institute of Technology, Cambridge, Massachusetts 02139, USA

[2]Veterans Affairs Boston Healthcare System and Harvard Medical School, Boston, MA

[3]Advanced Imaging Group, Thorlabs, Inc., Newton, NJ

[4]Praevium Research, Inc., Santa Barbara, CA

Introduction

Endoscopic imaging technologies such as confocal laser endomicroscopy (CLE)[1] and narrowband imaging (NBI)[2] have been used to investigate vascular changes as hallmarks of early cancer in the GI tract. However, the limited frame rate and field of view make CLE imaging sensitive to motion artifacts, whereas NBI has limited resolution and visualizes only the surface vascular pattern. Endoscopic optical coherence tomography (OCT) enables high speed volumetric imaging of subsurface features at near-microscopic resolution[3,4], and can image microvasculature without exogenous contrast agents[5] such as fluorescein, which obliterates the image in areas of bleeding, or after biopsies and resections. OCT has been demonstrated for visualizing microvasculature in small animal models[6] and larger vasculature in swine[3], however, the speed, resolution, and stability of previous systems were not sufficient for 3D visualization of microvasculature in endoscopic clinical applications[5]. Here, we present an ultrahigh speed endoscopic OCT technology that achieves >10 times faster imaging speed than commercial systems and high frame-to-frame stability, enabling OCT angiography in the human GI tract. Endoscopic OCT angiography of normal

Correspondence: Hiroshi Mashimo, MD, PhD, Gastroenterology Section, VA Boston Healthcare System, Harvard Medical School, Boston, MA, 02130, hmashimo@hms.harvard.edu, Telephone: +1-857-203-5640, Fax: +1-857-203-5666.
The work was performed at Veterans Affairs Boston Healthcare System.

Disclosures: JGF receives royalties from intellectual property owned by MIT and licensed to Carl Zeiss Meditec, Inc. and Lightlab Imaging/St. Jude Medical, Inc. JGF is a scientific advisor to and has stock options in Optovue.

Author Contributions: THT, JGF and HM designed the study; THT, OOA, YKT and BMP developed the instrumentation; VJ and AEC developed the high speed swept laser; THT, OOA, HCL, KL, MGG, and HM collected data; THT, OOA, MF and QH analyzed and interpreted data; JGF and HM obtained funding for the study; THT, OOA, JGF and HM wrote the manuscript; All authors read the manuscript; HM and JGF are principal investigators for this study.

esophagus, non-dysplastic Barrett's esophagus (BE) and normal recto-anal junction are demonstrated.

Description of Technology

An endoscopic OCT system with a 600 kHz[7] axial scan rate and a micromotor catheter were used to acquire circumferential, cross-sectional images at 400 frames per second. The combination of high axial scan rate and rotary speed provides densely sampled datasets with minimal motion artifacts, essential for performing endoscopic OCT angiography. Total image acquisition time was 8 seconds for each dataset, covering an area >100mm^2. The microvasculature contrast was generated by calculating the intensity decorrelation (D) between sequentially acquired images at a given voxel[8]. Decorrelation in the OCT signal intensity is caused by erythrocytes moving in the cross-sectional OCT image plane at a particular voxel. Voxels with high intensity variation yield higher decorrelation and are associated with flowing erythrocytes.

Video Description

A distal micromotor was used to rotate a reflecting micro-mirror. The OCT beam was reflected and focused outside of the catheter (**Video Clip 1**). By pulling back the imaging assembly, a helical OCT scan pattern was performed. Cross-sectional frames can be unwrapped to visualize different tissue ortho-planes. Microvasculature can be visualized without exogenous contrast by detecting the intensity decorrelation generated by moving erythrocytes.

The endoscopic OCT structural images of the normal esophagus show uniform *en face* features in the lamina propria (LP) layer and well-defined layered architecture, and corresponding OCT angiograms show 3D microvasculature (**Video Clip 2**). Vascular features are difficult to identify using structural images (Figure 1A & 1B). Endoscopic OCT angiography generates microvascular contrast, enabling visualization of the vessel network (Figure 1C). The cross-sectional OCT angiogram shows clear vascular features in the LP layer. High signal in the submucosa layer is due to the OCT beam diverging away from focal plane, so the spot size becomes too large to resolve individual vessels (Figure 1D). The endoscopic OCT images of a normal recto-anal junction show the dentate line separating rectum (columnar) and anal verge (squamous), delineated based on the subsurface structural features (Figure 1E). A corresponding OCT angiogram (Figure 1F) is generated from the same depth. A honeycomb-like vascular network around the crypts can be visualized on the rectum side, while little angiographic signal observed on the anal canal side, consistent with the structural differences between columnar and squamous epithelium.

Endoscopic OCT angiography was also performed in a patient with non-dysplastic BE (**Video Clip 2**, Figure 2A). The *en face* intensity image at a depth corresponding to the LP layer shows the SCJ can be delineated based on different structural features (Figure 2B). The left region exhibits atypical glandular structures consistent with BE. The enlarged view shows clear demarcation between normal (right) and BE (left) regions (Figure 2C). The cross-sectional OCT image across the SCJ shows BE mucosa adjacent to squamous mucosa, exhibiting glandular structure without significant distortion of the layered architecture.

Histology (Figure 2D) from the imaged region confirmed non-dysplastic BE. Figures 2E and 2F show *en face* endoscopic OCT angiograms at depths of the epithelium and LP layers, respectively. In Fig. 2E, a more prominent vascular network is present in the BE region, consistent with the surface vascular pattern typically observed in NBI images. The vasculature along the SCJ is denser than other regions, which may be a marker of disease progression. These results demonstrate that endoscopic OCT angiography can image the subsurface vascular pattern in BE and may provide valuable information for identification of premalignancy.

Take Home Message

Endoscopic OCT angiography enables visualization of 3D microvasculature in tissue without requiring exogenous contrast, augmenting the diagnostic capability of endoscopic OCT. The ability to visualize subsurface vasculature and structure is a unique feature of endoscopic OCT compared to CLE and NBI, which may improve detection of premalignant diseases in the GI tract. Furthermore, this capability may be beneficial for investigating other vascular diseases such as radiation proctitis, gastric antral vascular ectasia (GAVE), and ischemic colitis, as well as tumor-associated angiogenesis.

Acknowledgement

The authors gratefully acknowledge WooJhon Choi for suggesting angiographic imaging as well as Jonathan J. Liu and Chen D. Lu at MIT for helpful technical assistance and discussions. We also thank James Jiang, Jens Peupelmann, Peter J.S. Heim, Scott Jobling, Pak Cho, Changyi Lin, Alan Donaldson, John Hryniewicz, and Anjul Davis at Thorlabs, Inc. for technical support in the development of the high speed light source and OCT system.

Grant Support: National Institute of Health R01-CA75289-16, R44-CA101067-06, R44EY022864-01, R01-EY011289-27, R01-CA178636-01 and R01-HL095717-04; the Air Force Office of Scientific Research FA9550-12-1-0499 and FA9550-10-1-0551

References

1. Wallace M, et al. Endoscopy. 2011; 43:882–891. [PubMed: 21818734]
2. Sharma P, et al. Gastrointestinal Endoscopy. 2006; 64:167–175. [PubMed: 16860063]
3. Vakoc BJ, et al. Gastrointestinal Endoscopy. 2007; 65:898–905. [PubMed: 17383652]
4. Adler DC, et al. Nature Photonics. 2007; 1:709–716.
5. Yang VX, et al. Gastrointest Endosc. 2005; 61:879–890. [PubMed: 15933695]
6. Vakoc BJ, et al. Nature Medicine. 2009; 15:1219–U151.
7. Tsai TH, et al. Proc. SPIE 8927, Endoscopic Microscopy IX; Optical Techniques in Pulmonary Medicine. 2014; 89270T:1–6.
8. Jonathan E, et al. Journal of Biophotonics. 2011; 4:583–587. [PubMed: 21887769]

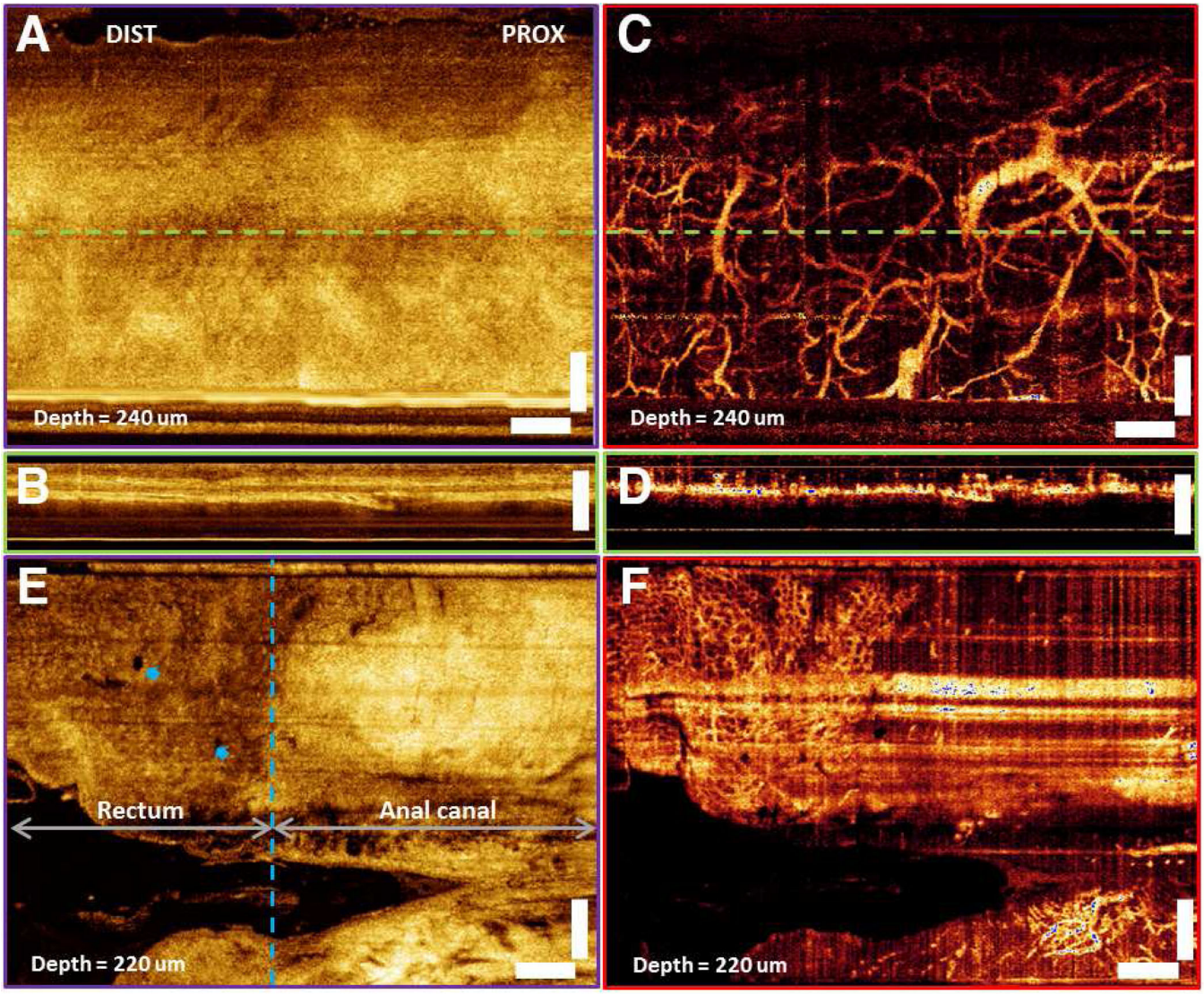

Figure 1.

Endoscopic OCT and angiography of normal esophagus (A-D) and recto-anal junction (E-F). (A) *En face* OCT image at 240μm depth (LP layer). (B) Cross-sectional OCT image along the pullback direction. (C) *En face* OCT angiogram in the LP layer. (D) Cross-sectional OCT angiogram along the pullback direction. (E) *En face* OCT image at 220μm depth (LP layer). (F) OCT angiogram shows the surface vasculature of the crypts in the rectum. Red arrows: anal glands; Blue arrows: rectal glands; White bar: 1mm.

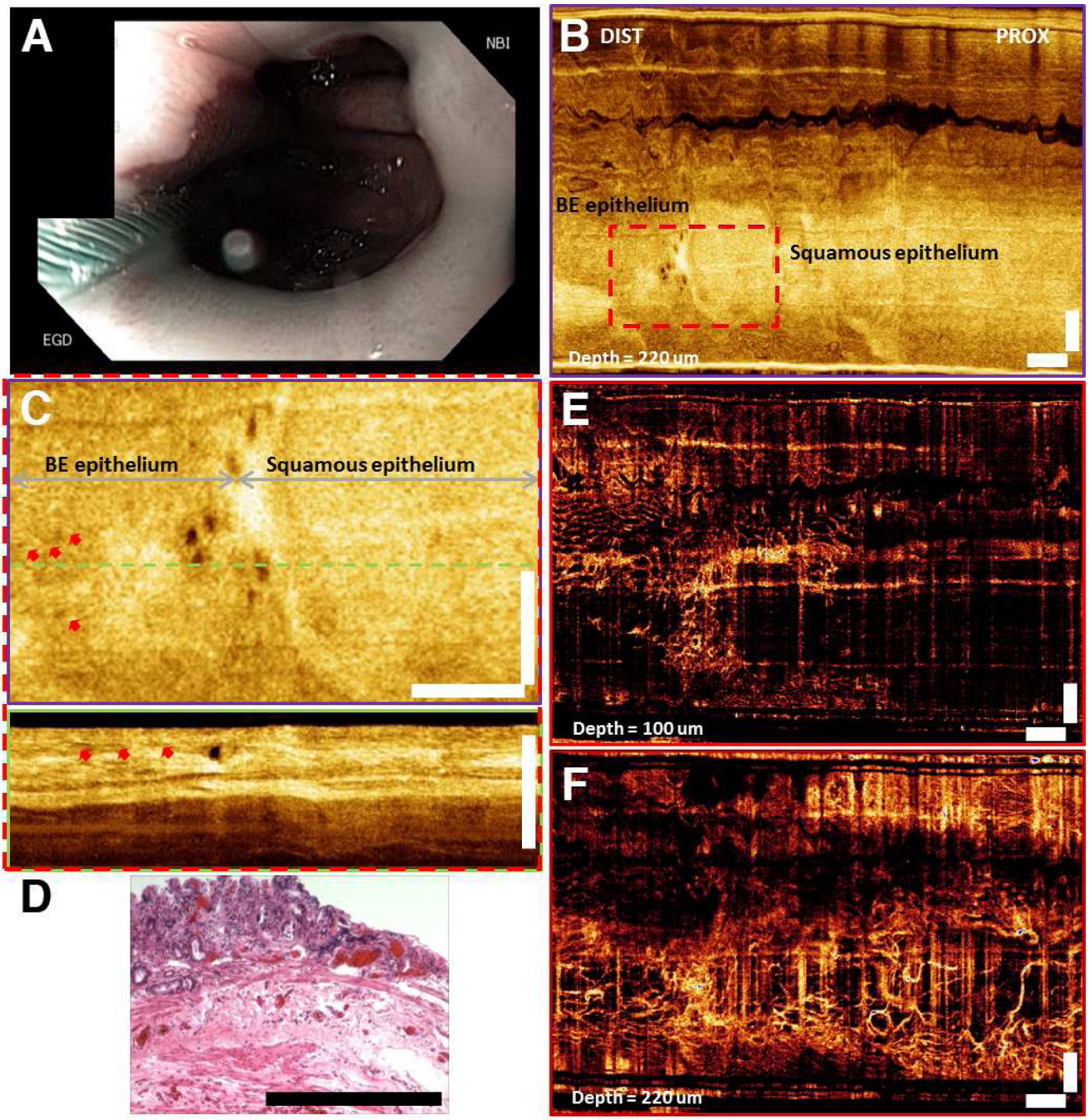

Figure 2.

Endoscopic OCT and angiography of Barrett's esophagus. (A) Endoscopic view of BE using NBI showing dark-red and irregular surface features. (B) *En face* OCT image at 220μm depth (LP layer). (C) Enlarged *en face* OCT image and the corresponding cross-sectional OCT image from the dashed red region in (B). (D) Corresponding histology from the imaged region. (E) *En face* OCT angiogram at 100μm depth showing surface vasculature in

the BE region. (F) *En face* OCT angiogram at 220μm depth showing high density of microvasculature along the SCJ. Red arrows: BE glands; White bar: 1mm.